RC 대형 냉각탑 셸의 손상추정에 관한 연구

A Study on Damage-Assessment of RC Large Cooling Tower Shells

노 삼 영*
Noh, Sam-Young

Abstract

An accumulated crack damage which propagates progressively with time was frequently observed on several engineering structures. This paper numerically demonstrates this damage process on large cooling tower shells under thermal and wind loads. Damage states under varying loads are investigated and the influence of this progressive damage process on the life-cycle of cooling towers discussed.

The paper presents briefly some fundamentals of the geometrically and physically non-linear numerical analysis employed for reinforced concrete, especially concerning the models used for concrete, steel reinforcement and the bond between them.

As a numerical example an existing cooling tower with noticeable meridian crack damage is analysed. The existing damage state of the cooling tower is determined by quasi-static analyses for temperature, hygric and cyclic wind loading. The change in the dynamical behaviour of the structure as mirrored in its natural frequencies and mode shapes is presented and discussed. Finally, the example shows that such damage processes develop progressively over the life-time of the structures.

Key words: cooling tower, reinforced concrete, crack, damage assessment

1. Introduction

Natural draught cooling towers are important components of power plants. Since they keep thermal pollution away from natural water bodies in the environment they regularly appear in thermal power plants all over the world. For increasing the thermal efficiency of power plants, natural draught cooling towers tend to become larger, that is higher, and thus they become more heavily exposed to wind loading. The world's largest cooling tower, constructed recently in Germany, is presented in [1] in detail.

It is well-known that cooling tower shells are subject to nearly continuous bending vibrations due to wind excitation. These bending vibrations significantly affect the behaviour of the structure and furthermore they are of particular importance for the tracing of the damage processes. Damage phenomena in cooling towers can be observed worldwide, in some cases even on recently constructed structures. Normally, after years of damage-free behaviour, visible cracks develop suddenly in the meridian direction of the shell. This crack-damage, initiated by thermal and hygric effects, grows progressively with time, as can also be observed on bridges under traffic and on offshore platforms under sea-wave excitation. The reason for these damage phenomena lies in a dynamic self-adaptation phenomenon of the structure moving towards higher excitation spectral values, after local initial damage

* 정회원, 한양대학교 건축학부 조교수

formation, thus producing a so-called damage-controlled structural self-adaptation ([2]).

The aim of this paper is a numerical demonstration of this progressive damage process of reinforced concrete shells in natural draught cooling towers. The final aim lies in improving the durability and extending the life-cycle of structures subject to such damage processes. The latter must be considered early in the design stage since repairs are difficult and maintenance and repair costs may become prohibitive. The most efficient way for reaching the above defined goal is therefore a durability- oriented design which takes into account the changing structural response under deterioration and damage processes.

2. Material modelling of reinforced conrete

2.1 General

Reinforced concrete is a composite material consisting of concrete and reinforcement steel and its load-carrying behaviour is highly non-linear. Characteristic properties of concrete are an essentially non-linear stress-strain relationship under mono tonic loading, yielding and damage development under cyclic loading in the compression domain and also cracking and crack closing processes in the tension domain. Compared to concrete, the elasto-plastic material law of reinforcing steel is quite simple. In addition, however, the complex non-linear bonding behaviour between concrete and steel as well as the tension-stiffening effect (participation of the concrete between cracks for monotonic and cyclic loading) are phenomena which must be considered.

Problems of lifetime assessment or lifetime extension typically require a rather involved nonlinear simulation of the structural damage processes. Here the capabilities of the material models employed for the realistic representation of the mechanical responses play a much more important role than in usual structural design applications, both in terms of phenomena description and parameter exactness. Thus the material behaviour should be modelled as accurately as possible. However, the experimental data on which the model validation is based are often ambiguous or their number is insufficient. It is, therefore, advisable to adjust the degree of model refinement to the problem at hand, in this case large scale r/c structures. Here, the material non-linearity is implemented by means of multi-layered model and, as shown in Fig. 1, the reinforced concrete in the tower shell is modelled as a layered continuum of uniaxial layers of reinforcement steel and of plane stress layers of concrete.

The used material model for the reinforced concrete is briefly summarized in the following, the description of the model in detail can be found in [13].

The concrete model used goes back to Darwin & Pecknold ([3]) and is a non-linear elasto-plastic damage model with material softening

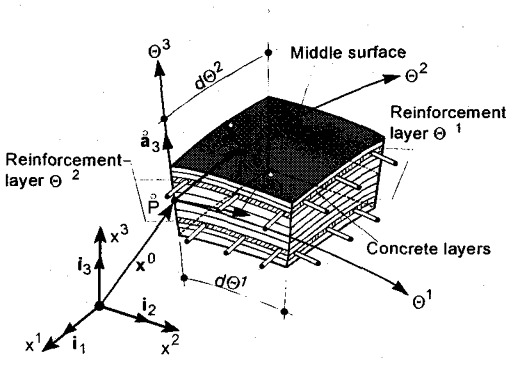

Fig.1 Multi-layered reinforced concrete shell model

2.2 Concrete in compression

The model is orthotropic in the principal stress directions for the biaxial state of stress. The characteristics of the formulation are as follows:

- Compact formulation by the introduction of an equivalent uniaxial strain.
- Applicability for monotonic and cyclic load processes with only four material parameters, namely the tension and com pression strengths, the strain for the compression strength and the initial YOUNG's modulus.
- Yield conditions are based on the experimental results of [4].
- Cyclic behaviour in compression is formulated based on the experimental data of [5] regarding degradation of strength and stiffness, yielding and energy dissipation.
- The ultimate failure criterion regarding material ductility depends on the compressive strength (0,2 σ_i) and strain of the concrete.

In the present work the ultimate failure condition is slightly modified in that the ultimate strain is defined for the compressive strength according to [6].

2.3 Reinforcement model and modification for considering the bond effect.

The reinforcement steel is idealized as smeared in the layered shell element pictured in Fig.1. In contrast to the concrete, reinforcement steel shows relatively simple material behaviour. In the present work the incremental uniaxial elasto-plastic constitutive law of Fig.3 is applied taking kinematic hardening due to Prager as well as the Bauschinger effect into account.

The bond between concrete and reinforcement plays an important role for the response of reinforced concrete structures under tension stresses. For the present investigation the bond effect is modelled indirectly as a participation of the concrete between the cracks (tension-stiffening) by modifying the steel model both for the monotonous and for the unidirectional cyclic loading ([8],[9]).

2.4 Description of the analysed cooling tower

In the numerical analysis the damage evolution in a large cooling tower shell and its spectral shifts under environmental loads were investigated. An existing tower, about 25 years old, with a pronounced crack pattern was chosen; Fig. 2 gives the dimensions and an impression of this structure with its varying shell thickness over the height. The cooling tower is characterized by the geometry of the hyperbolic shell described by equation (1)

$$r(z) = r_0 + \frac{a}{b}\sqrt{b^2 + (H_T - z)^2} \qquad (1)$$

with $r_0 = -23.6939\,m$, $a = 58.7739\,m$, $b = 121.6289\,m$ and $H_T = 118.0000\,m$.

The top lintel is constructed as a circular ring with $D/B = 0.30\,m/\,1.29\,m$. 50 V-columns with $D/B = 0.75\,m/\,0.90\,m$ support the shell.

The columns stand two by two on a foundation ($D/B/H = 4.00\,m/\,5.00\,m/\,1.50\,m$) which is simulated as a spring with an assumed WINKLER modulus of $k = 12.00\,MN/m^3$.

Fig.2 also depicts the existing reinforcement determined by linear analyses according to the design standard then in force. For the evaluation of the crack width, the diameter of the reinforcement employed ($8-16\,mm$) is simplified as $1\,mm$ uniformly. The material data for the used concrete and reinforcement steel can be found in Tab.1. For the reinforcement steel the tangent stiffness in the yield range is assumed 10^{-3} times the initial stiff ness E_0 and the fracture strain was defined as 0.1.The complete structure is modelled as a layered shell continuum consisting of 2 orthogonal uniaxial steel layers on both faces and 9 plane stress conrete

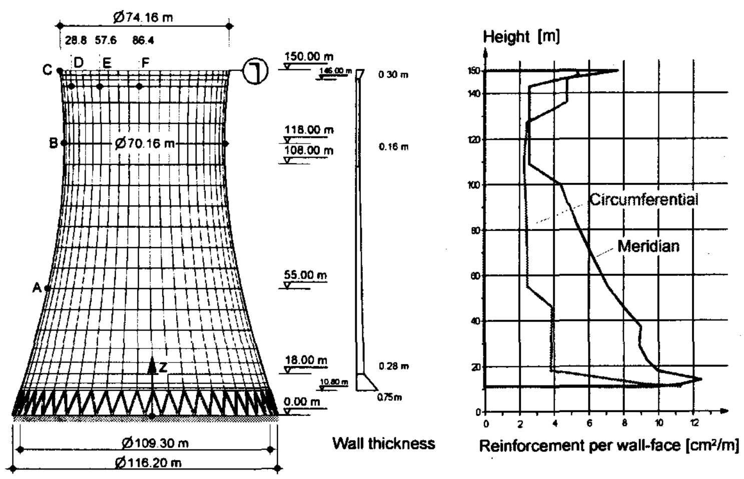

Fig.2 : Overview of the analysed cooling tower

Table 1: The material data for the used concrete and reinforcement steel

Concrete	sort	β_{W28} [MN/m2]	f_{ctm} [MN/m2]	E_0 [MN/m2]
Shell	BH 300	25.0	2.68	30000
Support	BH 450	40.0	2.92	35500
Foundation	BH 300	25.0	2,68	30000
Steel	sort	f_y [MN/m2]	f_t [MN/m2]	E_0 [MN/m2]
All	III	410.0	460.0	210000

layer. According to [10] the tower is subjected to the dead weight *G*, quasi-static wind load *W* of wind zone I with the wind pressure distribution curve K1.0 and alternatively to temperature loads due to winter service conditions with a temperature difference of 45 *K* from the cooler outer to the warmer inner face. In addition the hygric effect of swelling on the inner face due to permanent wetting and the shrinkage on the outer face were considered as a temperature load. A reasonable assumption according to [11] results in an equivalent tempera- ture gradient of 15 *K* for a nearly 30 years old tower.

2.5 Non-linear static analysis

Figs. 3 and 4 show the load-deflection curves at the investigated points B and E as shown in Fig. 2 for the three load cases. Without thermal service loads, the shell behaves linearly up to a wind load factor $\lambda = 1.75$. After this load level, cracks form and develop horizontally on the luff side as well as vertically on the flanks, successively. They propagate and join together with increasing wind load. Compared to that, the temperature load ΔT_{45K} under winter service condition leads to cracks on the whole outer face of the shell. The hygric effect increases the grade of this initial crack damage, leading particularly to circumferential bending damage in the flank regions. This initial damage tends however to be reduced with increasing wind load factor and finally the wind load alone determines the collapse behaviour of the tower. On this account, the tower collapses approximately at the same wind load factor of about $\lambda = 2.50$ in all three load cases investigated.

2.6 Natural frequency analysis

The stiffness reduction of structures during the

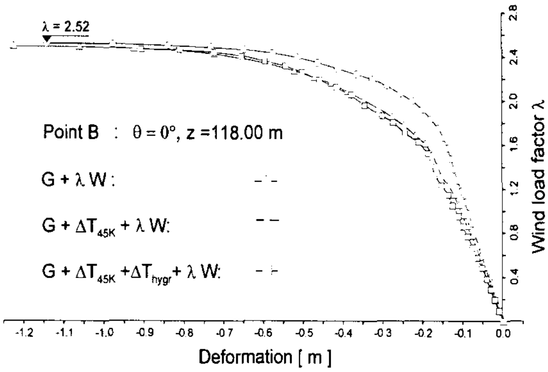

Fig.3: Load-deflection curves at point

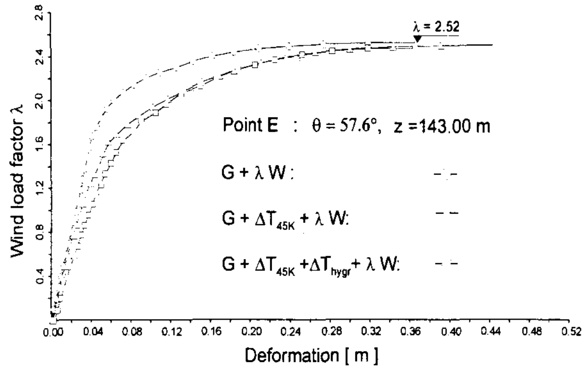

Fig. 4: Load-deflection curves at point E

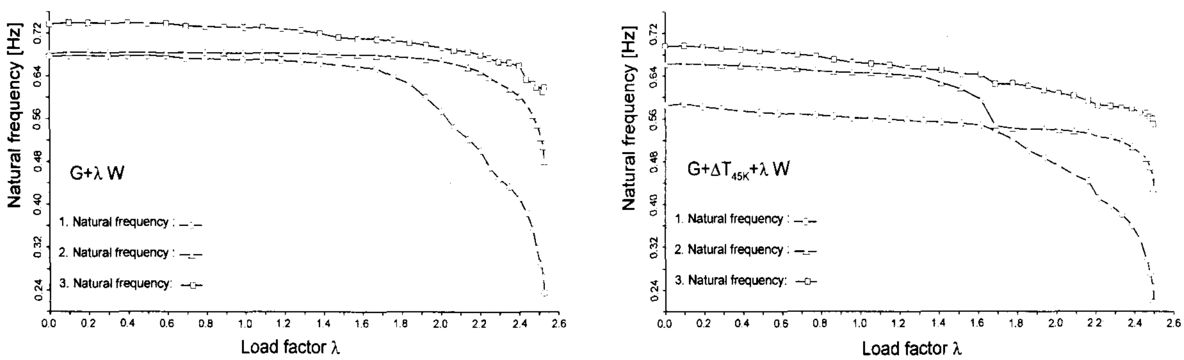

Fig.5: Shift of the first 3 natural frequencies under $G+\lambda W$ and $G+\Delta T_{45K}+\lambda W$

damage process influences its vibration charac teristics. In the numerical analysis this obviously affects the stiffness matrix K_T. The most succinct form of damage information in K_T corresponds to the structure's natural frequencies.

In the quasi-static analyses conducted above, the natural frequencies were also evaluated for the respective load states. Fig. 5 shows the shift of the first three natural frequencies as a function of the wind load factor λ, for the load cases with and without the initial damage induced by the temperature load. Under the load combination $G+\lambda W$ the three natural frequencies between $f=0.67Hz$ and $f=0.74Hz$ remain approximately constant up to the occurrence of the successive formation of horizontal cracks on the luff side at $\lambda=1.75$. Afterwards the first one drops drama tically until the collapse of the tower occurs, whereas both others remain nearly constant for much longer. The reduction of the stiffness due to temperature and hygric swelling decreases the natural frequencies considerably. The first natural frequency $f=0.67Hz$ reduces to $f=0.58Hz$ due to temperature load alone and to $f=0.49Hz$ under the additional hygric effect. Under the load combination $G+\Delta T_{45K}+\lambda W$ the second natural frequency reacts more strongly to variations in the wind load. Apparently, low wind loads do not affect the first natural frequency.

The shifted natural modes of the investigated damage states in Fig.6 indicate the changing dynamic properties of the structure in detail. The undamaged tower has its first three natural modes with 3, 5 and 4 waves respectively. However, after the formation of cracks on the whole outer face of the tower due to the temperature load, the new first mode with a natural frequency of $f=0.58Hz$ now has 5 waves, like the 2nd original mode. At the wind load level $\lambda=1.70$ at which the second natural frequency drops sharply, the second mode has 5

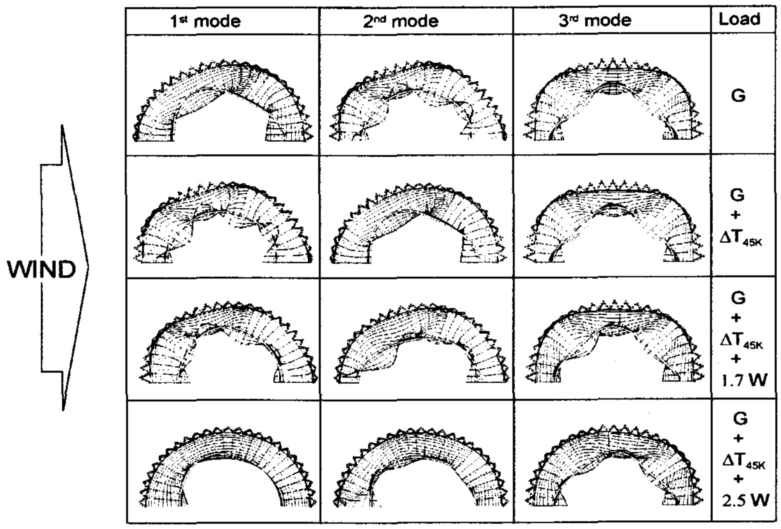

Fig.6 : Shift of the first 3 natural modes under $G + \Delta T_{45K} + \lambda W$

waves. From this load level onwards the first mode is quite similar to the real-life deformed figure of the structure. At a load level close to collapse ($\lambda = 2.50$), the second mode also assumes a similar form to the deformation of the structure. The evaluations of natural frequencies and natural modes under consideration of the hygric effect (reported in [12], [13]) show in principle the same behaviour.

2.7 Damage assessment

In order to quantify the generated global structural damage state, a set phenomenological damage indicators were defined from the set of natural frequencies f_i ([14], [15]). For a discretised structure with m degrees of freedom the damage

$$D_{fi}(\mathbf{V},d) = 1.00 - \frac{f_i(\mathbf{V},d)}{f_i(\mathbf{V}_0,d=0)} \qquad i = 1...m \tag{2}$$

indicators can be formulated as where $\mathbf{V}$ and d denote the nodal degrees of freedom vector and the damage state respectively.The difficulty arising in the practical application of the damage indicators D_{f1}, D_{f2}, etc. is that the number of significant natural frequencies have to be estimated in advance. The number generally depends on the structure and its loads. Another damage indicator $D_{\Delta V}$ has been defined in [16]

which has only one damage parameter, $\bar{f}_k$:

$$\bar{f}_k^{\,2} = \frac{\Delta\mathbf{V}_k^{0^T} \cdot \mathbf{K}_T \cdot \Delta\mathbf{V}_k^0}{\Delta\mathbf{V}_k^{0^T} \cdot \mathbf{M} \cdot \Delta\mathbf{V}_k^0} \tag{3}$$

This single indicator will now be compared with the indicators D_{fi}. The parameter $\bar{f}_k$ in equation (3) is based on the deformation increment $\Delta\mathbf{V}_k^0$ at the first iteration step of every load increment k - the so-called predictor. One obtains $\Delta\mathbf{V}_k^0$ from the incremental iteration of the equilibrium of the non-linear FE analysis and therefore this doesn't require any additional numerical effort. The damage parameter $\bar{f}_k$ is obtained by using the RAYLEIGH quotient in which the mode shape $\mathbf{\Phi}_k$ is substituted by the incremental deformation $\Delta\mathbf{V}_k^0$.

The damage indicator $D_{\Delta V}$ can be obtained using the same concept as for D_{fi} with the initial damage parameter $\bar{f}_0$ calculated for each load case:

$$D_{\Delta V}(\mathbf{V},d) = 1.00 - \frac{\bar{f}_k(\mathbf{V},d)}{\bar{f}_0(\mathbf{V}_0,d=0)} \tag{4}$$

The damage indicators D_{fi} based on the natural frequencies in Fig. 7 reflect the damage process in an effective way under both load combinations

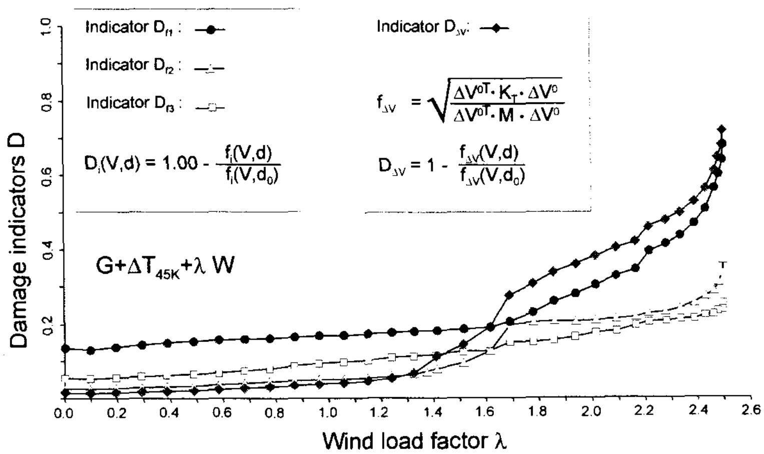

Fig.7 : Evolution of different damage indicators

$G+\lambda W$ and $G+\Delta T_{45K}+\lambda W$ as expected.

Compared to D_{f1}, $D_{\Delta V}$ indicates the damage process induced by the currently applied wind loads more accurately. Wind loads of intensity lower than $\lambda = 1.75$ damage only small areas of the shell. Therefore the values of $D_{\Delta V}$ stay under the global damage values of D_{f1} and the curve for $D_{\Delta V}$ is similar to the one for D_{f2}. After the wind load level $\lambda = 1.75$ is reached, the damage process due to wind dominates the global damage state of the shell and $D_{\Delta V}$ corresponds to D_{f1}. The application of both indicators allows the identification of the global damage state as well as of the damage process in the local area.

The determination of the evolution of natural frequencies during the damage process make it possible to estimate the increase of wind excitation level without time-consuming non-linear analyses. In Fig. 8 the first natural frequencies for some load cases are plotted into the VON- KARMAN spectrum.

In the standard spectrum, S denotes the spectral density function of the wind excitation, f the respective excitation frequencies and σ the variance. The figure clearly demonstrates the wind- and temperature-induced shifts of the first natural frequencies from their virgin positions towards the spectral peak. It is noticeable that the temperature and the hygric effect alone increase the dynamic excitation levels about 10 % and 25 % respectively.

Without any further non-linear dynamic computations one can thus deduce from the increase of the spectral excitation level an approximately equally large increase of the internal stresses.

3. Summary

In this paper damage processes of natural draught cooling towers were investigated. They were shown to be of the progressive damage type in agreement with the available evidence observed recently on different kinds of structures. The common features of these damage processes are the wide-band excitation present, a shift of the structural response spectrum towards higher excitations caused by degrading structural stiffness and also a damage-controlled self-adaptation phenomenon. The damage processes develop progressively over the life-cycle of the structure and cause a reduction of the originally expected life duration.

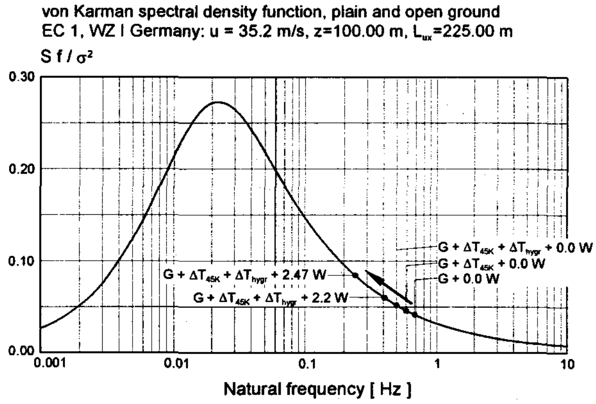

Fig.8 : Increase of wind dynamic excitation induced by damage

References

[1] W. B. Kraetzig, R. Harte, U. Montag, Computational concept for the durability design of the word's largest cooling tower shell, Edts.: H.A. Mang, F.G. Rammerstorfer,Fifth Word Congress on Computational Mechanics WCCM V, Vienna (2002).

[2] R. Harte, W. B. Kraetzig, S.-Y. Noh, Y. S. Petryna, On progressiv damage phenomena of structures, Computational Mechanics 25, 404-412, (2000).

[3] D. Darwin, D. A. Pecknold, Inelastic model for cyclic biaxial loading of reinforced concrete, Civil Engineering Studies SRS Nr. 409, University of Illinois (1974).

[4] H. B. Kupfer, H. K. Hilsdorf, H. Rsch, Behavior of concrete under Biaxial Stresses, ACI Journal 66(8), 656-666 (1969).

[5] I. D. Karsan, J. O. Jirsa, Behavior of concrete under compressive loadings, Journal of the Structural Division, ASCE, Vol 95(ST12), 2543-2563 (1969).

[6] MC90, CEB-FIP Model CODE 1990 Design Code, Bulletin d'Information 195, Comit Euro-International du Bton, Lausanne (1990).

[7] X. Su, B. Zhu, Algorithm for hysteresis analysis of prestressed-concrete frames, Journal of Structural Engineering Vol 120(6), 1732-1744 (1994).

[8] H. Kreller, Zum nichtlinearen Trag- und Verfor mungsverhalten von Stahlbetonstabtragwerken unter Last- und Zwangeinwirkung, Deutscher Ausschuss fuer Stahlbeton Heft 409 (1990).

[9] N. V. Tue, Zur Spannungsumlagerung im Spann beton bei der Rissbildung unter statischer und wiederholter Belastung, Deutscher Ausschuss fuer Stahlbeton Heft 435 (1993).

[10] VGB, BTR-Bautechnik bei kuehltuermen, VGB Technische Vereinigung der Grosskraftwerks-betreiber.

[11] DIN 4227, Spannbeton (1988).

[12] S.-Y. Noh, Beitrag zur numerischen Analyse der Schaedigungsmechanismen von Naturzug-kuehltuermen, Dr. -Ing. Thesis, RWTH, Department of Civil Engineering, Aachen, Germany (2001).

[13] W. B. Kraetzig, K. Meskouris, S.-Y. Noh, On damage process of natural draught cooling towers, Eds.: W.A. Wall et al., Trends in Computational Structural Mechanics, 338-347, CIMNE, Barcelona, Spain (2001).

[14] W. B. Kraetzig, Y. S. Petryna, Assessment of structural damage and failure, Archive of Applied Mechanics 71, 1-15 (2001).

[15] W. B. Kraetzig, Y. S. Petryna, F. Stangenberg, Mea sures of structural damage for global failure analysis, Int. J. Solids & Structures 37, 7393-7407 (2000).

[16] W. B. Kraetzig, S.-Y. Noh, F. Chen, Theorie und Simulation progressiver Schaedigungsprozesse von Naturzugkuehltuermen unter Wind- und Temperatureinwirkungen, Abschlussbericht des DFG-Forschungsprojektes Kr 350/27-2 (2000).